A Model for the Trap-Assisted Tunneling Mechanism in Diffused n-p and Implanted n^+-p HgCdTe Photodiodes

David Rosenfeld and Gad Bahir

Abstract—**In this paper we present a theoretical model for the trap-assisted tunneling process in diffused n-on-p and implanted n^+-on-p HgCdTe photodiodes. The model describes the connection between the leakage current associated with the traps and the trap characteristics: concentration, energy level, and capture cross sections. We have observed that the above two types of diodes differ in the voltage dependence of the trap-assisted tunneling current and dynamic resistance. Our model takes this difference into account and offers an explanation of the phenomenon. The good fit between measured and calculated dc characteristics of the photodiodes (for medium and high reverse bias and for temperatures from 65 to 140 K) supports the validity of the model.**

I. Introduction

THE MAIN interest in ternary alloys HgCdTe stems from their potential use in infrared detectors. One of the parameters affecting the performance of such devices is the trap concentration in the neutral as well as the depletion regions. Traps in the neutral region serve as Shockley-Read-Hall centers and bring about two short thermal transitions instead of one longer transition. They may cause a dramatic decrease in the minority-carrier lifetime in these regions [1]. The reduction of lifetime at a distance smaller than a diffusion length from the edge of the depletion region is of great importance, since it increases the diffusion leakage current and decreases the quantum efficiency as well as the photodiodes cutoff wavelength [2].

The role played by traps in the depletion region is more complicated. The existence of an electric field in the depletion region gives rise to two additional nonthermal transitions: a) tunneling of electrons from the valence band to the traps and b) tunneling from the traps to the conduction band. In addition to the thermal-thermal path that takes place in centers located in the neutral region, three more paths are possible in centers located within the depletion region: thermal-tunnel, tunnel-thermal, and tunnel-tunnel paths. The Shockley-Read-Hall mechanism is therefore replaced by a more complex mechanism, often called trap-assisted tunneling. The three additional paths add significant leakage current and therefore degrade the performance of photodiodes operated at low temperatures and reverse biases higher than 50 mV.

The negative effect of traps on the performance of HgCdTe diodes is not limited to the low-temperature high-bias region. In previously published works [3], [4] we demonstrated the correlation between tunneling currents and $1/f$ noise measured on HgCdTe diodes. It was shown that the low-frequency noise associated with tunneling mechanisms is much higher than that associated with diffusion and generation-recombination mechanisms. It was also found that the dark current of photodiodes, operated at the usual working conditions, is dominated by the diffusion mechanism, while the low-frequency noise is often dominated by tunneling mechanisms. The concentration and nature of the traps within the depletion region are therefore important parameters, which determine the low-frequency noise and may degrade the detector's signal-to-noise ratio, even when trap-assisted tunneling current is negligible.

Since each of the four paths involved in the trap-assisted tunneling process has different temperature and voltage dependencies, the overall temperature and voltage dependencies of the trap-assisted tunneling current is very complicated. Several published papers deal with the phenomena of trap-assisted tunneling in HgCdTe diodes [5]-[8] and capacitors [9]-[11], and present comparisons between theory and measured data. Most of these models seem to fit certain observed behavior within a limited range of operating conditions; namely, temperature and bias; but none in a wide range of these parameters. In this paper we model the trap-assisted tunneling current of front-illuminated diffused n-p and implanted n^+-p $Hg_{1-x}Cd_xTe$ photodiodes with $x \approx 0.22$. We compare measured and calculated characteristics in a wide range of temperatures (65-140 K) and biases (0.3-0.8 V). We also demonstrated the different voltage dependence of the trap-assisted tunneling mechanism in the high-temperature region and suggest an explanation for this difference.

Manuscript received February 18, 1991; revised December 20, 1991. The review of this paper was arranged by Associate Editor N. Moll.

D. Rosenfeld was with the Kidron Microelectronics Research Center, Department of Electrical Engineering, Technion—Israel Institute of Technology, Haifa 32000, Israel. He is now with NASA Lewis Research Center, Cleveland, OH 44135.

G. Bahir is with the Kidron Microelectronics Research Center, Department of Electrical Engineering, Technion—Israel Institute of Technology, Haifa 32000, Israel.

IEEE Log Number 9200386.

II. Device Processing and Surface Potential

The model and the measured data presented in the following sections characterize front-illuminated bulk HgCdTe photodiodes with $x \approx 0.22$. The starting material is undoped p-type bulk material grown by the traveling heater method (THM), either a) with $|N_A - N_D| \approx 10^{16}$ cm^{-3} at 77 K, or b) with $|N_A - N_D| \approx 3 \times 10^{17}$ cm^{-3} at 77 K.

In the case of the material with $N_A \approx 10^{16}$ cm^{-3}, n^+-p junctions were formed by implanting boron with a relatively low dose and low energy. The photodiodes were passivated with a thin film of native sulfides and covered with a 1-μm evaporated ZnS layer, which serves as an AR coating. After passivation the devices were exposed to a low-temperature post-implantation anneal (80°C). In the case of the heavily doped material ($N_A \approx 3 \times 10^{17}$ cm^{-3}), n-p diodes were fabricated by diffusing Hg into the bulk p. The n-p diodes were passivated with evaporated ZnS.

A small number of gate-controlled diodes and capacitors were fabricated near the n^+-p and n-p diodes. The gate-controlled diodes dc characteristics, as well as the capacitors C-V characteristics, were used to study the role played by the surface potential and to determine the relative contribution of surface-induced leakage currents. Using capacitors and gate-controlled diodes it has been shown that in properly processed passivated n^+-p [4], [12] and n-p [13] diodes, surface effects do not contribute significant dark current even at reverse biases as high as 1 V and temperature below 65 K. Hence, the model presented in the following section rightly ignores the negligible amount of surface-induced currents and concentrates on various leakage processes that take place in the bulk.

III. Modeling of the Trap-Assisted Tunneling Mechanism

In general, three distinct mechanisms dominate the leakage current and the dynamic resistance in HgCdTe diodes with $x \approx 0.22$: diffusion, band-to-band (direct) tunneling, and trap-assisted tunneling [4]. The diffusion mechanism dominates the leakage current and dynamic resistance in zero bias and low bias and in high temperatures. Band-to-band tunneling is the dominant leakage mechanism in high reverse biases and low temperatures, in diodes fabricated on doped material. Trap-assisted tunneling is the dominant mechanism in medium biases and medium temperature regions in diodes fabricated on doped material, and in wider regions in diodes realized on undoped material. It has been lately shown by Nemirovsky *et al.* [4], [12] that the trap-assisted tunneling dominates the current and dynamic resistance in HgCdTe diodes fabricated on undoped material even in temperatures down to 65 K and reverse biases up to 1 V.

Modeling of the trap-assisted tunneling mechanism is rather complicated since the dc characteristics are mostly defined by the nature of the depletion region. The current and dynamic resistance are determined by the concentration of traps in the depletion region, by their distance from the edges of the bands, by their capture cross section, and by the depletion-region doping level. Since in both ion-implanted and diffused HgCdTe diodes the doping level and the trap concentration may depend on the distance from the junction—a simple model describing the voltage dependence of that mechanism will not be accurate. Modeling of the temperature dependence is even more complicated since the temperature behavior of the capture cross section depends on the origin of the material and on the type of trap and therefore may vary with each sample.

Fig. 1 shows the energy bands of a diode with a mid-gap level in high (Fig. 1(a)) and low (Fig. 1(b)) reverse biases. It is clearly seen that thermal transitions are always possible for all traps while tunnel transitions are not. An essential condition for the electron tunneling process is a trap energy "higher" than the bottom of the conduction band. Similarly, holes can tunnel from a trap to the valence band only if the trap energy is "lower" than the top of the valence band. Fig. 1 shows that traps can be divided into four major groups according to the following allowed carrier transitions:

a) Traps that can exchange carriers with the valence band by thermal transition only, and with the conduction band using both thermal and tunnel transitions.

b) Traps that can exchange carriers with both bands using thermal transitions only (Shockley–Read–Hall centers).

c) Traps that can exchange carriers with the valence band by thermal and tunnel transitions, and with the conduction band by thermal transition only.

d) Traps that can exchange carriers with both bands by thermal and tunnel transitions.

In the case of degenerate n^+-p diodes, two additional groups of traps are added (see Fig. 2):

e) Traps with thermal and tunnel transitions such as (c), but with a higher thermal barrier due to the Burstein–Moss shift.

f) Traps with only thermal transitions such as (b), but with a higher thermal barrier due to the Burstein–Moss shift.

Since each group has its characteristic carrier transition paths, each is associated with different occupation probability as well as with different probabilities for tunnel and thermal transitions, and hence different contributions to the overall current. In addition, the relative number of traps associated with each group depends strongly on temperature and bias. For example: the trap-assisted tunneling current in a diode with mid-gap traps operated at high reverse bias is dominated by the contribution of group (d), while in the case of low reverse bias the contribution of that group is negligible (see Fig. 1). Hence, modeling of the trap-assisted tunneling current should include detailed calculations of the relative concentration of traps in each group as well as their special characteristics.

The different role played by the two types of holes shoule be noted. Since the tunneling rate of carriers is inversely proportional to the exponent of their mass, the tunneling probability of heavy holes is much smaller than

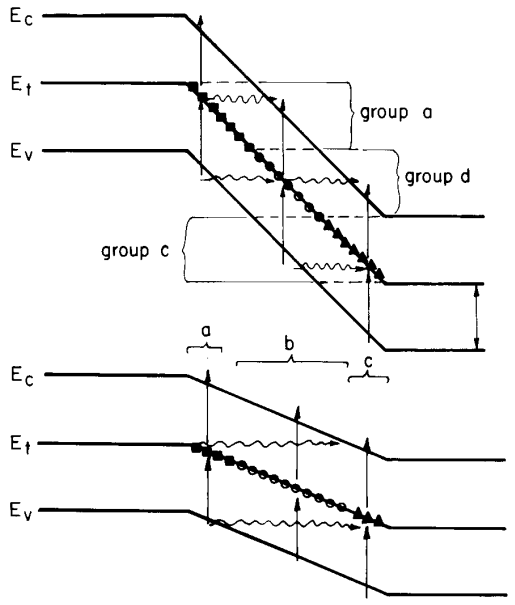

Fig. 1. The energy bands of an n-p diode with a mid-gap trap level in high (upper) and low (lower) reverse biases. The traps are divided into four major groups according to the allowed carrier transitions.

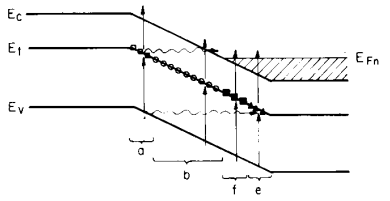

Fig. 2. The energy bands of an n^+-p diode. Two additional groups of traps, (e) and (f), are added due to the Burstein-Moss shift.

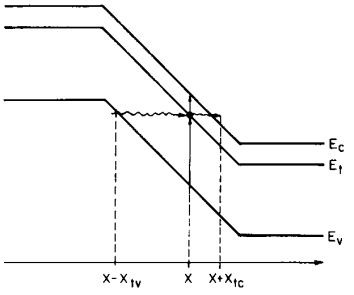

Fig. 3. The four transitions of group (d) and the tunneling distances.

that of light ones and therefore can be ignored. On the other hand, due to the higher density of states in the heavy-hole band, the thermal transition of heavy holes is much higher than that of light ones. As a result, the hole thermal transition is dominated by heavy holes while the hole tunnel transition is dominated by light ones.

Let us consider the generation-recombination transition path of group (d) in which all tunnel and thermal transitions are allowed. The net capture rate of electrons into centers located at a distance x from the junction and with energy E_T and concentration N_{Td} is

$$U_{nd} = \gamma_n n(x) N_{Td}(1 - f) - \gamma_n n_1 N_{Td} f + \omega_c n(x + x_{tc}) N_{Td}(1 - f) - N_C \omega_c N_{Td} f \quad (1)$$

and the net capture rate of holes into the same traps is

$$U_{pd} = \gamma_p p_h(x) N_{Td} f - \gamma_p p_1 N_{Td}(1 - f) + \omega_v p_L(x - x_{tv}) N_{Td} f - \omega_v N_v N_{Td}(1 - f) \quad (2)$$

where x_{tc} and x_{tv} are the tunneling distances for electrons and holes (see Fig. 3)), and $f = f(x)$ is the trap occupation probability. γ_p and γ_n are the electron and holes capture coefficients, p_h, p_L, and n are the concentration of heavy holes, light holes, and electrons, and N_V and N_C are the light holes and the electron effective densities of states. ω_c and ω_v represent the carriers tunneling probabilities between the center and the bands. The temperature dependence of the thermal emission rates is given by $n_1 = N_C \cdot \exp(-(E_g - E_T)/kT)$ for electrons and by $p_1 = N_{Vh} \cdot \exp(-E_T/kT)$ for heavy holes (where N_{Vh} is their effective density of states).

Assuming quasi-equilibrium situation, $U_{nd} = U_{pd}$, $n \cdot p_h = n_i^2 \cdot \exp(qV/kT)$, and $n, p_L, p_h \to 0$ in the depletion region, the net generation rate of group (d) U_d is given by

$$U_d = N_{Td}\left[\frac{-\gamma_n\gamma_p n_i^2(e^{(qV/kT)} - 1) + \omega_c N_C \omega_v N_V + \gamma_n n_1 \omega_v N_V + \gamma_p p_1 \omega_c N_C}{\gamma_n n_1 + \gamma_p p_1 + \omega_c N_C + \omega_v N_V}\right]. \quad (3)$$

The net generation rates of groups (a), (b), and (c) can be easily obtained using (3). Assuming $\omega_v N_V \to 0$ for group (a), $\omega_v N_V \to 0$, $\omega_c N_C \to 0$ for group (b), and $\omega_c N_C \to 0$ for group (c) one obtains

$$U_a = N_{Ta}\left[\frac{-\gamma_n\gamma_p n_i^2(e^{(qV/kT)} - 1) + \gamma_p p_1 \omega_c N_C}{\gamma_n n_1 + \gamma_p p_1 + \omega_c N_C}\right] \quad (4)$$

$$U_b = N_{Tb}\left[\frac{-\gamma_n\gamma_p n_i^2(e^{(qV/kT)} - 1)}{\gamma_n n_1 + \gamma_p p_1}\right] \quad (5)$$

$$U_c = N_{Tc}\left[\frac{-\gamma_n\gamma_p n_i^2(e^{(qV/kT)} - 1) + \gamma_n n_1 \omega_v N_V}{\gamma_n n_1 + \gamma_p p_1 + \omega_v N_V}\right] \quad (6)$$

where N_{Ta}, N_{Tb}, and N_{Tc} represent the concentration of traps in groups (a), (b), and (c), respectively.

The net generation rates of group (e) and (f) (shown in Fig. 2), can also be obtained by replacing the electron thermal barrier $(E_g - E_T)$ with $(E_g - E_T + BS)$, where BS is the average additional barrier caused by the Burstein-Moss effect. The temperature dependence of the

thermal emission rate is given now by

$$n_2 = N_C \exp\left[\frac{-(E_g - E_T + BS)}{kT}\right] = n_1 e^{(-BS/kT)} \tag{7}$$

and the generation rates (of N_{Te} traps in group (e) and N_{Tf} traps in group (f)) by

$$U_e = N_{Te}\left[\frac{-\gamma_n\gamma_p n_i^2(e^{(qV/kT)} - 1) + \gamma_n n_i \omega_v N_V}{\gamma_n n_1 e^{(BS/kT)} + \gamma_p p_1 + \omega_v N_V}\right] \cdot e^{(BS/kT)} \tag{8}$$

$$U_f = N_{Tf}\left[\frac{-\gamma_n\gamma_p n_i^2(e^{(qV/kT)} - 1)}{\gamma_n n_1 + \gamma_p p_1 e^{(-BS/kT)}}\right]. \tag{9}$$

The magnitude of the tunneling rates $\omega_c N_C$ and $\omega_v N_V$ are obviously important in determining the trap-assisted tunneling current. The tunnel diode theory of Sah [14] indicates that the tunneling rates out of a group of traps located at a distance E_T from the valence band are given by

$$\omega_c N_C = \frac{\pi^2 q m_c^* E M^2}{h^3(E_g - E_T)} \cdot \exp\left[\frac{-8\pi(2m_c^*)^{1/2}(E_g - E_T)^{3/2}}{3hqE}\right] \tag{10}$$

$$\omega_v N_V = \frac{\pi^2 q m_v^* E M^2}{h^3 E_T} \cdot \exp\left[\frac{-8\pi(2m_v^*)^{1/2}E_T^{3/2}}{3hqE}\right] \tag{11}$$

where E is the maximum electric field in the depletion region, M is the matrix element of the trap potential energy, and m_v^* and m_c^* are the effective masses of carriers in the valence and conduction bands. The tunneling probability of light holes is much greater than that of heavy holes and therefore is the only probability to be considered. Following Kinch [9], we assume that the effective masses of light holes and electrons are given by $m_v^* = m_c^* = 0.07 m_0 E_g$, where m_0 is the electron rest mass and E_g is the bandgap in electron-volts. We use the experimentally determined value [9] for $m_v^* M^2 = m_c^* M^2 = 10^{-23}$ V · cm^3 and finally obtain

$$\omega_c N_C = \frac{6 \times 10^5 E}{E_g - E_T} \cdot \exp\left[\frac{-1.7 \times 10^7 E_g^{1/2}(E_g - E_T)^{3/2}}{E}\right] \tag{12}$$

$$\omega_v N_V = \frac{6 \times 10^5 E}{E_T} \cdot \exp\left[\frac{-1.7 \times 10^7 E_g^{1/2} E_T^{3/2}}{E}\right]. \tag{13}$$

The magnitude and temperature dependence of the capture coefficients are also important in determining the trap-assisted tunneling current. In general, the capture coefficients γ_p and γ_n are given by

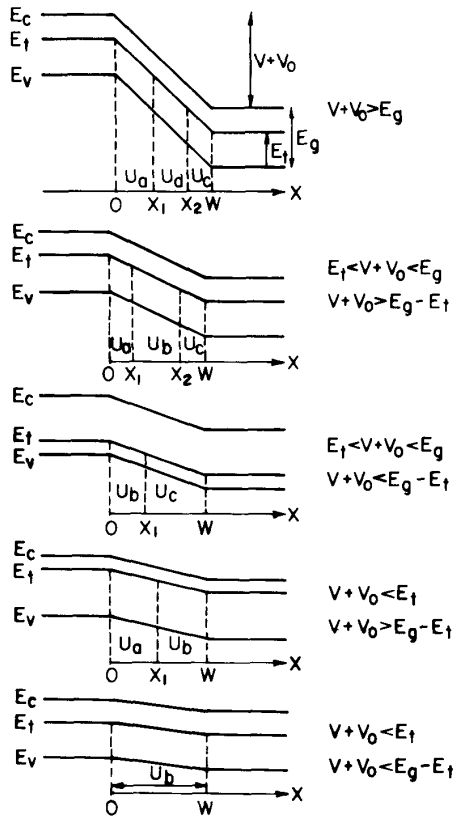

Fig. 4. The energy bands of an n-p diode and the five possible relations (between V, V_0, E_g, and E_T), as well as the various groups of traps and their position within the depletion region.

$$\gamma_p = \sigma_p V_{tp} \qquad \gamma_n = \sigma_n V_{tn} \tag{14}$$

$$V_{tp} = \left[\frac{kT}{3m_{vh}^*}\right]^{1/2} \qquad v_{tn} = \left[\frac{kT}{3m_c^*}\right]^{1/2} \tag{15}$$

$$m_{vh}^* = 0.55 \cdot m_0 \qquad m_c^* = 0.07 \cdot m_0 \cdot E_g$$

where σ_p, σ_n, V_{tp}, V_{tn}, m_{vh}^*, and m_c^* are capture cross sections, thermal velocities, and effective masses of heavy holes and electrons, respectively. Since the two effective masses are linear functions of the temperature we can use Lax estimation [15] for the temperature dependence of electron and hole capture cross sections $\sigma_n \propto T^{-\delta n}$ and $\sigma_p \propto T^{-\delta p}$, and estimate the temperature dependence of electron and hole capture coefficients to be

$$\gamma_p(T) = \gamma_{p0}\left[\frac{T}{77}\right]^{-\beta_p} \tag{17a}$$

$$\gamma_n(T) = \gamma_{n0}\left[\frac{T}{77}\right]^{-\beta_n} \tag{17b}$$

where γ_{p0} and γ_{n0} are the capture coefficients at 77 K and β_p and β_n are fitting parameters.

The overall trap-assisted tunneling current can now be obtained by integrating the net generation rate across the depletion region. To do so one should take into account the generation rate and the number of traps associated with each group.

Detailed calculations of energy bands in p-type HgCdTe which take into account the high density of states in the valence band show that for 60 K $< T <$ 150 K the material does not become degenerate even with doping levels higher than 10^{18} cm^{-3}. Therefore, in the case of n-p diodes the traps can be divided into four groups. The relative number of traps in each group is determined by the relations between the built-in voltage, the applied voltage, the bandgap, and the energy level of the traps.

Fig. 4 shows the five significant relations possible in n-p diodes as well as the various groups of traps and their position within the depletion region. By integrating the net generation rate across the depletion region we obtain the total generation rate in each one of the five cases

$$U = \begin{cases} \displaystyle\int_0^{W(E_T/(V+V_0))} U_a\,dx + \int_{W(E_T/(V+V_0))}^{W(1-(E_g-E_T)/(V+V_0))} + \int_{W(1-(E_g-E_T)/(V+V_0))}^{W} U_c\,dx, & V+V_0 > E_g \\ \displaystyle\int_0^{W(1-(E_g-E_T)/(V+V_0))} U_a\,dx + \int_{W(1-(E_g-E_T)/(V+V_0))}^{W(E_T/(V+V_0))} U_d\,dx + \int_{W(E_T/V+V_0)}^{W} U_c\,dx, & E_T < V+V_0 < E_g,\ V+V_0 > E_g - E_T \\ \displaystyle\int_0^{W(E_T/(V+V_0))} U_b\,dx + \int_{W(E_T/(V+V_0))}^{W} U_c\,dx, & E_T < V+V_0 < E_g,\ V+V_0 < E_g - E_T \\ \displaystyle\int_0^{W(1-(E_g-E_T)/(V+V_0))} U_a\,dx + \int_{W(1-(E_g-E_T)/(V+V_0))}^{W} U_b\,dx, & V+V_0 < E_T,\ V+V_0 > E_g - E_T \\ \displaystyle\int_0^{W} U_b\,dx, & V+V_0 < E_T,\ V+V_0 < E_g - E_T. \end{cases} \tag{18}$$

Since U_a, U_b, U_c, and U_d are constant, the integration yields

$$J_{TAT} = \begin{cases} qW \cdot N_T \cdot \left(U_a\left(\dfrac{E_T}{V+V_0}\right) + U_d\left(1 - \dfrac{E_g}{V+V_0}\right) + U_c\left(\dfrac{E_g - E_T}{V+V_0}\right)\right), & V+V_0 > E_g \\ qW \cdot N_T \cdot \left(U_a\left(1 - \dfrac{E_g - E_T}{V+V_0}\right) + U_b\left(\dfrac{E_g}{V+V_0} - 1\right) + U_c\left(1 - \dfrac{E_T}{V+V_0}\right)\right), & E_T < V+V_0 < E_g,\ V+V_0 > E_g - E_T \\ qW \cdot N_T \cdot \left(U_b\left(\dfrac{E_T}{V+V_0}\right) + U_c\left(1 - \dfrac{E_T}{V+V_0}\right)\right), & E_T < V+V_0 < E_g,\ V+V_0 < E_g - E_T \\ qW \cdot N_T \cdot \left(U_a\left(1 - \dfrac{E_g - E_T}{V+V_0}\right) + U_b\left(\dfrac{E_g - E_T}{V+V_0}\right)\right), & V+V_0 < E_T,\ V+V_0 > E_g - E_T \\ qW \cdot N_T \cdot U_b, & V+V_0 < E_T,\ V+V_0 < E_g - E_T \end{cases} \tag{19}$$

pletion region. The total generation rate for $V_0 + V > E_g + BS$ is given now by

$$U = \int_0^{W(E_T/(V-V_0))} U_a\,dx + \int_{W(E_T/(V+V_0))}^{W(1-(E_g-E_T+BS)/(V+V_0))} U_d\,dx + \int_{W(1-(E_g-E_T+BS)/(V+V_0))}^{W(1-BS/(V+V_0))} U_c\,dx + \int_{W(1-BS/(V+V_0))}^{W} U_e\,dx. \tag{20a}$$

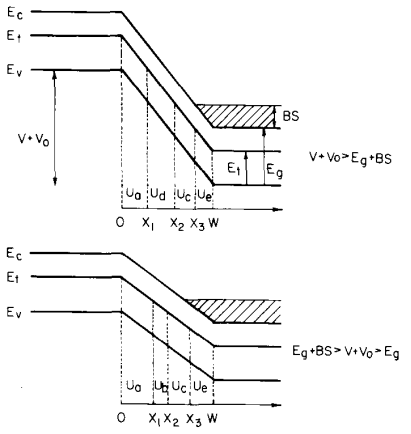

Fig. 5. The energy bands of an n^+-p diode and the two relations between V, V_0, E_g, E_T, and BS, possible for reverse bias above 50 mV. The various groups of traps and their position within the depletion region are also plotted.

Similarly, for $E_g < V_0 + V < E_g + BS$ the net generation rate is given by

$$U = \int_0^{W(1-(E_g-E_T-BS)/(V+V_0))} U_a\,dx + \int_{W(1-(E_g-E_T-BS)/(V+V_0))}^{W(E_T/(V+V_0))} U_d\,dx + \int_{W(E_T/(V+V_0))}^{W(1-BS/(V+V_0))} U_c\,dx + \int_{W(1-BS/(V+V_0))}^{W} U_e\,dx. \tag{20b}$$

The associated trap-assisted tunneling current J_{TAT} is now given by

$$J_{TAT} = qWN_T\left[U_a\left(\frac{E_T}{V+V_0}\right) + U_d\left(1-\frac{E_g+BS}{V+V_0}\right) + U_c\left(\frac{E_g-E_T}{V+V_0}\right) + U_e\left(\frac{BS}{V+V_0}\right)\right] \tag{21a}$$

for $V_0 + V > E_g + BS$, and for $E_g < V_0 + V < E_g + BS$ by

$$J_{TAT} = qWN_T\left[U_a\left(1-\frac{E_g+BS-E_T}{V+V_0}\right) + U_b\cdot\left(\frac{E_g+BS}{V+V_0}-1\right) + U_c\left(1-\frac{E_T+BS}{V+V_0}\right) + U_e\left(\frac{BS}{V+V_0}\right)\right]. \tag{21b}$$

IV. Results and Discussion

Figs. 6 and 7 represent typical resistance-temperature characteristics (R-T) of two one-sided HgCdTe photodiodes fabricated on undoped THM material. We chose to compare measured and calculated resistance instead of currents because small changes in the characteristics become evident. Being the derivative of the current, the dynamic resistance reveals small changes that are masked in the current characteristics.

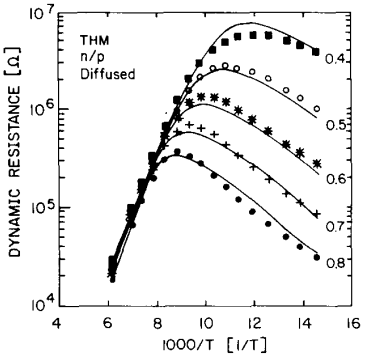

Fig. 6. Measured and calculated characteristics of a diffused n-p diode with $x = 0.219$, $N_D = 2 \times 10^{15}$ cm^{-3}, and junction area of $A_j = 2 \times 10^{-5}$ cm^2. The dynamic resistance associated with the trap-assisted tunneling mechanism versus reciprocal temperature is plotted, with the diode reverse bias as a parameter. The symbols represent measured data while the solid curves represent theory. The fit was obtained for $N_T = 4.3 \times 10^{16}$ cm^{-3}, $E_T = 0.6E_g$, $\gamma_{n0} = 3.2 \times 10^{-7}$ [cm^3/S], $\beta_n = 1$, $\gamma_{p0} = 9.8 \times 10^{-7}$ [cm^3/S], and $\beta_p = 0.3$.

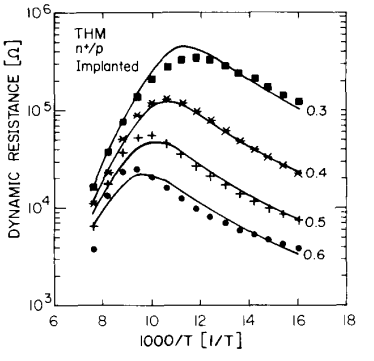

Fig. 7. Measured and calculated characteristics of an ion-implanted n^+-p diode with $x = 0.225$, $N_A = 10^{16}$ cm^{-3}, and junction area of $A_j = 2 \times 10^{-5}$ cm^2. The dynamic resistance associated with the trap-assisted tunneling mechanism versus reciprocal temperature is plotted, with the diode reverse bias as a parameter. The symbols represent measured data while the solid curves represent theory. The fit was obtained for $E_T = 0.6E_g$, $\gamma_{n0} = 2.1 \times 10^{-6}$ [cm^3/S], $\beta_n = 1.3$, $\gamma_{p0} = 6.6 \times 10^{-5}$ [cm^3/S], and $\beta_p = 0.3$. The effective trap concentration for $V = 0.6$ V is $N_T = 1.8 \times 10^{16}$ cm^{-3}. For smaller bias we multiply both the carrier concentration and the traps concentration by a factor $\eta < 1$, maintaining the same ratio between the trap and acceptor concentrations. The obtained values for η were 0.93, 0.86, and 0.78 for reverse biases of $V = 0.5$, 0.4, and 0.3 V, respectively.

Fig. 6 shows the characteristics of a representative diffused n-p diode with $x = 0.219$ and $n = 2 \times 10^{15}$ cm^{-3} (at 77 K). Fig. 7 shows the characteristics of an implanted n^+-p diode with $x = 0.225$ and $p = 10^{16}$ cm^{-3} (at 77 K). The two figures show dynamic resistance versus reciprocal temperature, with the diode's reverse bias as a parameter. The symbols represent measured data while the solid curves represent the theoretical model presented in (3)–(21); namely, the numerical derivatives of (19) and

(21). As indicated by Nemirovsky *et al.* [4], in the entire temperature and bias regions of Figs. 6 and 7, the leakage current and dynamic resistance of undoped diodes are dominated by the trap-assisted tunneling mechanism. Therefore, our calculations of leakage current disregard the contribution of other leakage mechanisms such as diffusion and band-to-band tunneling.

The complex temperature dependence of the trap-assisted tunneling process is seen clearly in both figures. The high-temperature regions are dominated by Shockely–Read–Hall thermal–thermal transitions as indicated by straight lines on a semilog scale. The low-temperature regions, on the other hand, are dominated by the tunnel–tunnel transitions as indicated by the decrease in the dynamic resistance with decreasing temperature.

In addition to the difference in the average resistances, caused mainly by the different compositions, the two diodes differ in their voltage dependence in the high-temperature region. The diffused n-p diode represented in Fig. 6 exhibits almost no voltage dependence in the region dominated by thermal–thermal transitions. Fig. 7, on the other hand, demonstrates the strong voltage dependence of the dynamic resistance of the n^+-p implanted photodiode in the same temperature region. This last figure shows that the dynamic resistance is degraded by a factor of 5, as the reverse bias is increased from 300 to 600 mV. This is unexpected behavior since both current and dynamic resistance in this temperature region are dominated by thermal–thermal transitions and therefore should exhibit negligible field dependence. The suggested explanation for this behavior is related to the profile of vacancies close to the junction, and will be discussed in the next paragraph.

Tobin [16] and Riley [17] have both observed a linear relationship between the shallow acceptor concentration due to Hg vacancy and the deep trap concentration. They have suggested that the traps are either a different (and additional) state of the Hg vacancy or a complex involving the Hg vacancy. Both Tobin and Riley did not rule out either the additional vacancy-state model or the vacancy-complex model. However, the correlation between trap and vacancy concentrations they observed is of great importance, since it indicates that the vacancies produce both the shallow level (responsible for p-type conductivity) and the deep level (traps). Also, it has been found and demonstrated by Bubulac *et al.* [18], that in undoped material, Hg freed by the implant annihilates vacancies and decreases the doping level in the region adjacent to the n^+ region. Fraenkel *et al.* [19], and more recently Nemirovsky *et al.* [4], used *C–V* profiling techniques to characterize the carrier profile of HgCdTe photodiodes realized by implanting boron into undoped material. They have found that n^+-p^--p junctions are formed with very low p doping near the junction, and that the doping increases gradually until it reaches the bulk doping level. In order to explain the thermal–thermal transitions voltage dependence in implanted diodes we rely on these two phenomena. By considering the gradual profile of the Hg vacancy and the correlation between vacancy and trap concentrations, we suggest that the trap concentration is gradual as well. Therefore, as the reverse bias increases and the depletion region expands, regions with higher trap concentration are introduced and the average number of traps increases. As a result, even in temperature regions dominated by thermal–thermal transitions, the trap-assisted tunneling current and dynamic resistance depend strongly on bias.

The good fit between measured and calculated dynamic resistance of the two diodes supports the validity of the model as demonstrated in Figs. 6 and 7. In the case of a diffused n-p photodiode, the fit was obtained for trap energy of $E_T = 0.6E_g$ and trap concentration of $N_T = 4.3 \times 10^{16}$ cm^{-3}. The obtained values of the electron capture coefficients were $\gamma_{n0} = 3.2 \times 10^{-7}$ [cm^3/S] and $\beta_n = 1$ and the hole capture coefficients were $\gamma_{p0} = 9.8 \times 10^{-7}$ [cm^3/S] and $\beta_p = 0.3$. Using (14)–(16) the capture cross sections at 77 K were calculated to be $\sigma_n = 4.7 \times 10^{-15}$ cm^2 and $\sigma_p = 1.2 \times 10^{-13}$ cm^2.

In the case of implanted n^+-p photodiodes, a good fit was obtained for trap energy of $E_T = 0.75E_g$. Since the vacancy concentration (and therefore the carrier concentration as well) was assumed to depend on the distance from the junction in these diodes, different effective carrier and trap concentrations for each bias were used. The values derived from the fitting process for $V = 0.6$ V were $N_T = 1.8 \times 10^{16}$ cm^{-3} and $N_A = 10^{16}$ cm^{-3}. For smaller bias values we multiply both the acceptor concentration and the trap concentration by a factor $\eta < 1$, maintaining the same ratio between trap and acceptor concentrations. The obtained values for η were 0.93, 0.86, and 0.78 for reverse biases of $V = 0.5$, 0.4, and 0.3 V, respectively. The attained values of the electron capture coefficients were $\gamma_{n0} = 2.1 \times 10^{-6}$ [cm^3/S] and $\beta_n = 1.3$ and that of holes were $\gamma_{p0} = 6.6 \times 10^{-5}$ [cm^3/S] and $\beta_p = 0.3$. The capture cross sections calculated using (14)–(16), were $\sigma_n = 3.3 \times 10^{-14}$ cm^2 and $\sigma_p = 8.2 \times 10^{-12}$ cm^2 at 77 K, for the electrons and the holes, respectively.

The values for trap energy levels, concentrations, and capture cross sections, obtained from the fit between measured and calculated characteristics, are in agreement with those published in the literature, mostly by Polla, Jones and co-authors [20]–[22]. In this work data on traps in undoped HgCdTe based on DLTS measurements were provided. Although they have reported the existence of two energy levels associated with the deep traps $0.4E_g$ and $0.75E_g$, they have found that only the $0.75E_g$ level determines the *R–T* characteristics [22]. The trap concentrations reported by them ranged from approximately $0.1N_A$ to $10N_A$ (where N_A is the shallow acceptor concentration), and therefore are also in agreement with our values. However, our results differ from previously published values since we obtained acceptor-like centers with $\sigma_p > \sigma_n$. Such centers with $\sigma_p > \sigma_n$ were found only in As doped material [23].

V. Summary

In this paper we modeled the trap-assisted tunneling mechanism of n-p and n^+-p $Hg_{1-x}Cd_xTe$ photodiodes. The model describes the connection between the leakage current and dynamic resistance associated with the traps, the trap characteristics (energy level, concentration, and capture cross sections), and the bulk properties (dopant concentration and composition). We demonstrated the difference between these two types of photodiodes in the voltage dependence of the trap-assisted tunneling current and resistance, and suggested an explanation for this difference. Finally, we supported the validity of the model by comparing measured and calculated characteristics in a wide range of temperatures (65–140 K) and biases (0.3–0.8 V). Good fits between measured and calculated characteristics were obtained for trap concentrations, energy levels, and capture cross sections, close to those presented in the literature. Unfortunately, only a handful of published works [20]–[23] deal with the nature of traps in undoped HgCdTe. Therefore, the validity of our model should be farther confirmed, by replacing the published characteristics of the traps with DLTS data measured on our samples [24]. In addition, more detailed studies of the trap profile and their connection with the shallow acceptor level are needed.

Acknowledgment

The authors wish to thank the scientific team at Semi-Conductor Devices, Jerusalem, Israel, for the fabrication of the diodes of Fig. 7. The authors are grateful to E. Haugland from NASA Lewis Research Center, and to S. E. Schacham from the Department of Electrical Engineering at Technion for their useful remarks. The technical assistance of D. Schoenmann, A. Zohar, N. Steinbrecher, S. Dolev, P. Elyaou, and Y. Betser from the Kidron Microelectronics Research Center are also acknowledged with thanks. Special thanks are given to I. Rosenfeld and R. Rosenfeld for their editorial assistance.

References

[1] M. B. Reine, A. K. Sood, and T. J. Tredwell, "Photovoltaic detectors," in *Semiconductors and Semimetals*, vol. 18, R. K. Willarson and A. C. Beer, Eds. New York: Academic Press, 1981, ch. 6.

[2] Y. Nemirovsky and D. Rosenfeld, "The cut-off wavelength and minority carrier lifetime in implanted n^+ on bulk p HgCdTe photodiodes," *J. Appl. Phys.*, vol. 83, no. 7, no. 1, p. 2435, 1988.

[3] D. Rosenfeld and Y. Nemirovsky, "Tunneling induced 1/f noise in HgCdTe photodiodes," presented at The 16th Conf. of Electrical and Electronics Engineering in Israel, Convention Center, Tel-Aviv Grounds, Israel, Mar. 7–9, 1989.

[4] Y. Nemirovsky, D. Rosenfeld, R. Adar, and A. Kornfeld, "Tunneling and dark currents in HgCdTe photodiodes," *J. Vac. Sci. Technol. A*, vol. 7, p. 529, 1989.

[5] R. E. Dewames, J. G. Pasko, E. S. Yao, A. H. B. Vanderwyck, and G. M. Williams, "Dark current generation mechanisms and spectral noise current in long-wavelength infrared photodiodes," *J. Vac. Sci., Technol. A*, vol. 6, p. 2655, 1988.

[6] R. E. Dewames, G. M. Williams, J. G. Pasko, and A. H. B. Vanderwyck, "Current generation mechanisms in small band gap HgCdTe pn fabricated by ion implantation," *J. Crystal Growth*, vol. 86, p. 948, 1988.

[7] Y. Nemirovsky, R. Fastow, M. Meyassed, and A. Unikovsky, accepted for publication in *J. Vac. Sci. Technol.*, Apr. 1991.

[8] W. W. Anderson and J. Hoffman, "Field ionization of deep levels in semiconductors with applications to HgCdTe pn junctions," *J. Appl. Phys.*, vol. 53, p. 9130, 1982.

[9] M. A. Kinch, "Metal insulator semiconductor infrared detectors," in *Semiconductors and Semimetals*, vol. 18, R. K. Willarson and A. C. Beer, Eds. New York: Academic Press, 1981, ch. 7.

[10] D. K. Blanks, J.D. Beck, M. A. Kinch, and L. Colombo, "Band-to-band processes in HgCdTe: Comparison of experimental and theoretical studies," *J. Vac. Sci. Technol. A*, vol. 6, p. 2790, 1988.

[11] P. Omaggio, "Analysis of dark current in IR detectors on thinned p-typed HgCdTe," *IEEE Trans. Electron Devices*, vol. 37, no. 1, pp. 141–152, 1990.

[12] Y. Nemirovsky and D. Rosenfeld, "Surface passivation and 1/f noise phenomena in HgCdTe photodiodes," *J. Vac. Sci. Technol. A*, vo. 8, p. 1159, 1990.

[13] D. Rosenfeld and G. Bahir, to be published.

[14] C. T. Sah, "Electronic processes and excess currents in gold-doped narrow junctions," *Phys. Rev.*, vol. 109, p. 1594, 1958.

[15] M. Lax, "Cascade capture of electrons in solids," *Phys. Rev.*, vol. 119, p. 1502, 1960.

[16] S. P. Tobin, M.S. thesis, MIT, 1979.

[17] K. J. Reily, P. R. Pratt, and A. H. Lockwood, in *IRIS Meet. of the Specialty Groups on Infrared Detectors and Imaging*, vol. 1, p. 333, 1978.

[18] L. O. Bubulac and W. E. Tennant, "Role of Hg in junction formation in ion-implanted HgCdTe," *Appl. Phys. Lett.*, vol. 51, p. 355, 1987.

[19] A. Fraenkel, S. E. Schacham, G. Bahir, and E. Finkman, "Lifetime and carrier concentration profiles of B implanted p-type HgCdTe," *J. Appl. Phys.*, vol. 60, p. 3916, 1986.

[20] D. L. Polla and C. E. Jones, "Deep level studies of HgCdTe. I: Narrow bandgap space charge spectroscopy," *J. Appl. Phys.*, vol. 52, no. 8, p. 5118, 1981.

[21] D. L. Polla, M. B. Reine, and C. E. Jones, "Deep level studies of HgCdTe. II: Correlation with photodiode performance," *J. Appl. Phys.*, vol. 52, no. 8, p. 5132, 1981.

[22] C. E. Jones, V. Nair, and D. L. Polla, "Generation-recombination centers in p-type HgCdTe," *Appl. Phys. Lett.*, vol. 39, no. 3, p. 248, 1981.

[23] C. E. Jones, *et al.*, "Status of point defects in HgCdTe," *J. Vac. Sci. Technol.*, vol. A3, no. 1, p. 131, 1985.

[24] S. J. Zackman, M.Sc. thesis, Technion, Haifa, Israel, to be published.

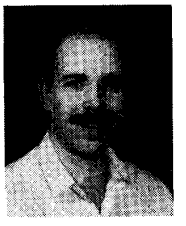

David Rosenfeld was born in Mexico City, Mexico, on December 4, 1957. He received the B.Sc., M.Sc., and D.Sc. degrees in electrical engineering from the Technion—Israel Institute of Technology, Haifa, Israel in 1983, 1985, and 1989, respectively.

In 1989 he joined the Kidron Microelectronics Research Center at the Technion, where he was involved with the fabrication and characterization of infrared detectors. Currently, he is holding a National Research Council Fellowship and researching the properties of Si/Ge heterostructures at NASA Lewis Research Center, Cleveland, OH.

Gad Bahir was born in Israel. In 1969 he graduated from the Hebrew University of Jerusalem, Jerusalem, Israel, with the B.Sc. degree in physics and mathematics. He received the M.Sc. and D.Sc. degrees in physics from the Technion—Israel Institute of Technology, Haifa, Israel, in 1976 and 1982.

From 1982 to 1984 he was a Research Fellow at the Microelectronics Research Center of the Technion, working on narrow-bandgap semiconductors and IR detectors. From 1984 to 1987 he was employed as a Visiting Scientist at the Department of Electrical Engineering in the University of California at Santa Barbara, working on InP technology. Since 1987 he has been with the Department of Electrical Engineering at the Technion, where he is currently working on quantum wells IR detectors and compound semiconductor technology.